Enhancement of narrow-band terahertz radiation from photoconducting antennas by optical pulse shaping

Yongqian Liu, Sang-Gyu Park, and A. M. Weiner

School of Electrical and Computer Engineering, Purdue University, West Lafayette, Indiana 47907-1285

Received July 5, 1996

We report the use of optical pulse shaping to convert single femtosecond pulses into lower-intensity pulse sequences for excitation of photoconductive dipole antennas, which results in the generation of bursts of tunable narrow-band free-space terahertz radiation. Our experiments demonstrate that the use of such pulse sequences can significantly enhance the spectral amplitude of the narrow-band terahertz radiation by avoiding the saturation effects that occur with single-pulse excitation. Our technique also provides the capability for terahertz wave-form shaping. © 1996 Optical Society of America

Generation of ultrafast bursts of terahertz (THz) radiation propagating in free space has attracted considerable attention in recent years.[1–3] In the most common generation technique, broadband THz radiation is produced as a result of ultrafast current surges excited in photoconductive switches by single femtosecond optical pulses.[1–3] THz free-space radiation has been used in applications in coherent time-domain spectroscopy,[2] in imaging and ranging of objects,[3,4] and as a diagnostic of ultrafast carrier dynamics in semiconductors.[5,6] On the other hand, some applications, such as radar and microwave communications and far-infrared nonlinear optics, favor high power, and sometimes narrow-band, THz radiation. For this reason a number of researchers have investigated the optimum design of photoconductive THz transmitters and the physical mechanisms that limit the radiation power.[7–9] In addition, generation of tunable narrow-band THz radiation was recently demonstrated by use of a train of femtosecond excitation pulses derived from the interference between a pair of highly chirped optical pulses.[10] In this Letter we report generation of narrow-band THz radiation from a photoconducting antenna driven by optical pulse sequences obtained through femtosecond pulse shaping.[11–13] Our experiments demonstrate, for the first time to our knowledge, that the power spectral density at the peak of the narrow-band THz spectrum can be significantly enhanced by the use of multiple-pulse sequences. We attribute these surprising results to the avoidance of saturation effects, which can occur, for example, when the radiated field amplitude is sufficient to partially screen the applied bias field.

In our experiment a Ti:sapphire oscillator produced ~100-fs input pulses at a repetition rate of 80 MHz centered around a wavelength of 800 nm. These input pulses passed through a grating-and-lens optical pulse shaper.[11–13] A spatially patterned, periodic phase mask was placed in the Fourier plane of the pulse shaper to tailor the optical frequency spectrum. This mask is similar to that used previously for impulsive excitation of coherent phonons in molecular crystals[13] and coherent control of charge oscillations in semiconductor heterostructures.[6] The pulse repetition rate could be tuned from 750 GHz to 1.3 THz by selection of mask patterns with different spatial periodicities. The excitation pulse sequence was focused to an ~10-μm spot on the transmitting antenna. The antenna, mounted upon a Si hyperhemispherical substrate lens, was a dc-biased photoconducting dipole antenna fabricated upon low-temperature (LT) GaAs with a subpicosecond carrier lifetime.[14] In our experiment a 25-V bias was applied across a 5-μm photoconductive gap. The THz radiation propagated in free space and was focused by another Si hyperhemispherical lens onto a similar photoconducting dipole antenna, which acted as the receiver. The receiver was placed ~10 cm away from the transmitter to detect the far-field radiation. A portion (~40 mW) of a split beam from the original pulse was used as a trigger to sample the THz radiation sensed by the detector. The current signal, proportional to the radiated field, was amplified by a current preamplifier and recorded by a lock-in amplifier. We mapped out the THz radiation field as a function of time by varying the delay between the excitation pulse and the sampling pulse.

Figures 1(a) and 1(b) show intensity cross-correlation measurements of the optical excitation pulses made with a single unshaped pulse split off from the laser as a reference. Cross-correlation measurements are shown both for single excitation pulses obtained by removing the mask pattern from the pulse shaper [Fig. 1(a)] and for a 750-GHz multiple pulse sequence [Fig. 1(b)]. Figures 1(c) and 1(d) show measurements of the THz radiation generated by the single-pulse and the multiple-pulse sequences at a fixed 44-mW average pump power. Excitation with the pulse sequence resulted in a quasi-sinusoidal THz waveform with a center frequency equal to the repetition frequency of the optical pulse train. The multiple-pulse sequence functions as an active filter to select a particular THz radiation frequency. One can easily tune the center frequency of the narrow-band THz radiation by varying the spatial period of the mask patterns, which changes the optical pulse repetition frequency.

Here we are particularly interested in comparing the amplitude of THz radiation generated by single- and multiple-optical-pulse excitation. One can show that, if the photoconducting antenna remains in the linear

0146-9592/96/211762-03$10.00/0

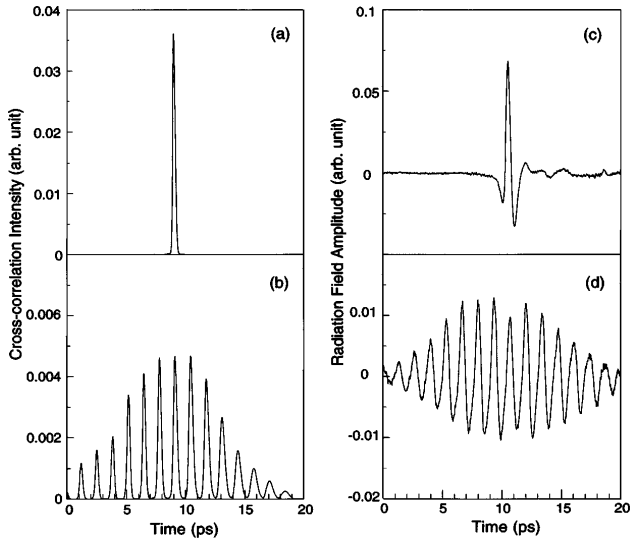

Fig. 1. Intensity cross-correlation measurement of the input optical excitation pulse: (a) single pulse, (b) multiple pulses. Time-domain waveforms for the THz radiation using (c) single-optical-pulse and (d) multiple-optical-pulse excitation.

response regime, the peak THz spectral amplitude at frequency ν_0 excited by a multiple-pulse sequence with repetition rate ν_0 is the same as the THz spectral amplitude at frequency ν_0 that results from single-pulse excitation, provided that the overall optical fluence is unchanged. Thus, even though use of a multiple-pulse sequence diminishes the peak optical intensity and the peak THz field as viewed in the time domain, the multiple-pulse character of the resultant waveforms leads to the same THz spectral amplitude at the selected frequency. This is indeed the case in our experiments at low optical powers ($P < 12$ mW). However, for higher optical power a dramatic difference between single-pulse and multiple-pulse excitation is observed. To compare the power dependence of the THz radiation for these two cases, we performed fast Fourier transforms (FFT's) of the measured THz time-domain waveforms. Figure 2 shows the FFT field spectrum for a high-excitation case at an average optical power of 44 mW. The peak THz spectral amplitude observed at the first-harmonic frequency $\nu_0 = 750$ GHz resulting from multiple-pulse excitation is increased by a factor of $\sim$1.84 compared with that for single-pulse excitation. This corresponds to a factor-of-$\sim$3.4 enhancement in the power spectral density. Also evident are the second- and third-harmonic radiation from the multiple-pulse excitation; however, at these high frequencies the enhancement relative to the single-pulse results is clearly reduced. This frequency-dependent enhancement of narrow-band THz generation by use of multiple-pulse optical excitation arises because of the avoidance of saturation mechanisms that limit the THz amplitude in the case of high-power single-optical-pulse excitation.

Figure 3 is a plot representing the THz spectral amplitude at $\nu_0 = 750$ GHz as a function of average optical power for both single- and multiple-pulse excitation. The filled symbols in the plot are derived directly from the FFT of the measured THz time-domain waveforms; we obtained the open symbols simply by recording the peak amplitudes of the detected time-domain THz waveforms versus power and then multiplying by the appropriate scale factors to convert from peak time-domain amplitude to spectral amplitude at ν_0. We determined the scale factor by comparing the THz time-domain data and their Fourier transforms for 44-mW average pump power for both single- and multiple-pulse excitation. The same scale factors (one for single pulses and one for multiple pulses) were then applied to generate the amplitudes represented by all the open symbols. Both single- and multiple-pulse plots show a linear dependence on optical power for average powers below $\sim$12 mW. At higher powers, however, the THz amplitude for single-pulse excitation saturates, whereas the THz signal obtained by multiple-pulse excitation remains linear with optical power. The avoidance of saturation in the latter case arises because the peak optical intensity of the multiple-pulse sequence is reduced nearly tenfold

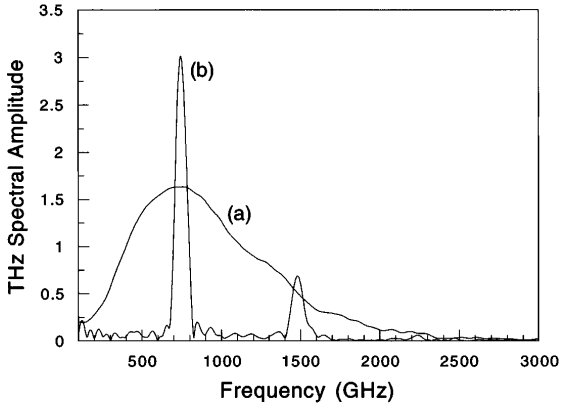

Fig. 2. Field spectrum of the THz radiation generated with (a) single-pulse and (b) multiple-pulse excitation at an average power of 44 mW.

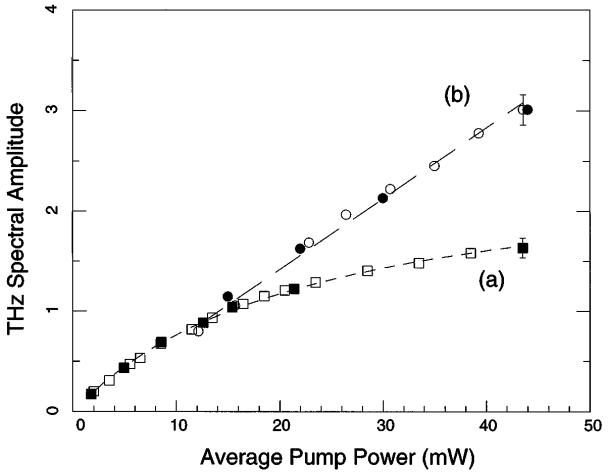

Fig. 3. Spectral amplitudes of the THz radiation as a function of the average excitation powers for the (a) single- and (b) multiple-optical pulse excitations. Filled symbols represent peak spectral amplitudes obtained directly from FFT's. Open symbols represent peak amplitudes in the time domain scaled to the spectral amplitudes at ν_0 by multiplication by the appropriate scale factors. Dashed curves are fits to relation (1) for (a) $F_s \sim 350$ μJ/cm^2; (b) is a linear fit. Also shown are typical error bars.

compared with that of the original single pulse, thus scaling multiple-pulse excitation into the linear response regime.

The scaling and saturation behavior of THz radiation with single-optical-pulse excitation has been studied both experimentally and theoretically.[5,7–9,15] In principle, the saturation at high optical power densities could result from screening of the bias field either owing to the space-charge field or owing to the radiation field itself. Saturation studies of dipole antennas and related structures have focused on space-charge screening, which has led to significant saturation on an ultrafast time scale at carrier densities in the $10^{17}-10^{18}$-cm^{-3} range.[5,15] In our highest-power (44-mW) single-pulse experiments the estimated carrier density is 3×10^{18} cm^{-3}. This suggests that space-charge screening may also play a role in our single-pulse experiments, even though the magnitude of these effects will depend on the precise device geometry. With multiple-pulse excitation each individual pulse generates substantially fewer electron–hole pairs. Provided that the space-charge relaxation time is faster than the pulse repetition period (as is likely given the subpicosecond carrier lifetime of our LT-GaAs transmitter), screening effects that are due to the space-charge field are strongly reduced with multiple pulses. Our observation that the enhancement obtained with multiple pulses appears to be frequency dependent (see Fig. 2) may point to the presence of a finite saturation recovery time, which could serve as a signature for contributions of space-charge screening to the saturation behavior. Further investigations will be needed to elucidate this point.

In the case of large-aperture antennas, attention has focused on screening of the bias field by the radiation field. The THz field expected when saturation is due to screening by the radiation field is given by the following formula, valid when the aperture is large compared with the shortest THz wavelength[7,8]:

$$E_r(t) \sim -E_b \frac{F_{\mathrm{opt}}/F_s}{1 + F_{\mathrm{opt}}/F_s}. \qquad (1)$$

Here E_b is the bias field, F_{opt} is the optical fluence, and the saturation fluence F_{s} is a constant. Our experiments use fluences as high as 700 μJ/cm^2, well above the saturation fluences reported for large-aperture antennas[7,8]; a fit to our single-pulse data by relation (1) with $F_s = 350$ μJ/cm^2 shows good agreement with our experimental results [Fig. 3(a), dashed curve]. Thus it seems likely that screening by the radiation field may be an important effect in our experiments, even though the large-aperture results do not directly apply to our setup, for which the dipole size is much less than the average THz average wavelength. In the experiments using multiple-pulse excitation the saturation is linked to peak optical power (or fluence per individual pulse). Spreading the optical excitation into multiple pulses, resulting in a reduced peak radiation field, greatly extends the saturation regime.

Our current research does not distinguish between space-charge field and radiation field screening mechanisms, although multiple-pulse excitation appears capable of alleviating both mechanisms. It may be possible to further distinguish between these potential saturation mechanisms by performing experiments in which both the pulse sequences and the material parameters are varied. In particular, studies of the saturation behavior as a function of pulse repetition rate and carrier lifetime should shed light on the relative contributions of these saturation mechanisms. Furthermore, we note that, although the use of dipole antennas has limited the absolute field amplitude achieved in our current study, our proof-of-principle results can be extended to enhance THz power spectral densities achieved with high-power large-aperture antennas.

In conclusion, we have observed an enhancement of narrow-band THz radiation by using a femtosecond pulse shaper to generate optical pulse sequences used to excite a photoconducting antenna. This technique can be extended to generate tunable, narrow-band THz radiation or specially crafted, programmable THz waveforms with the addition of a programmable optical pulse shaper for THz waveform engineering.

We acknowledge helpful discussions with J. F. Whitaker and fabrication of the pulse shaping mask by D. E. Leaird. This research was supported by the National Science Foundation under grant 9404677-PHY and by the U.S. Air Force Office of Scientific Research under contract AFOSR F49620-95-1-0490.

References

1. P. R. Smith, D. H. Auston, and M. C. Nuss, IEEE J. Quantum Electron. **24,** 255 (1988).
2. D. Grischkowsky, S. Keiding, M. van Exter, and Ch. Fattinger, J. Opt. Soc. Am. B **7,** 2006 (1990).
3. B. B. Hu and M. C. Nuss, Opt. Lett. **20,** 1716 (1995).
4. R. A. Cheville and D. Grischkowsky, Appl. Phys. Lett. **67,** 1960 (1995).
5. W. Sha, J. Rhee, T. Norris, and W. J. Schaff, IEEE J. Quantum Electron. **28,** 2445 (1992).
6. I. Brener, P. C. M. Planken, M. C. Nuss, M. S. C. Luo, S. L. Chuang, L. Pfeiffer, D. E. Leaird, and A. M. Weiner, J. Opt. Soc. Am. B **11,** 2457 (1994).
7. J. T. Darrow, X.-C. Zhang, D. H. Auston, and J. D. Morse, IEEE J. Quantum Electron. **28,** 1607 (1992).
8. P. K. Benicewicz, J. P. Roberts, and A. J. Taylor, J. Opt. Soc. Am. B **11,** 2533 (1994).
9. B. I. Greene, J. F. Federici, D. R. Dykaar, R. R. Jones, and P. H. Bucksbaum, Appl. Phys. Lett. **59,** 893 (1991).
10. A. S. Weling, B. B. Hu, N. M. Froberg, and D. H. Auston, Appl. Phys. Lett. **64,** 137 (1994).
11. A. M. Weiner, J. P. Heritage, and E. M. Kirschner, J. Opt. Soc. Am. B **5,** 1563 (1988).
12. A. M. Weiner, D. E. Leaird, J. S. Patel, and J. R. Wullert, IEEE J. Quantum Electron. **28,** 908 (1992).
13. A. M. Weiner, D. E. Leaird, G. P. Wiederrecht, and K. A. Nelson, Science **247,** 1317 (1990).
14. S. Gupta, M. Frankel, J. A. Valdmanis, J. F. Whitaker, G. Mourou, F. W. Smith, and A. R. Calawa, Appl. Phys. Lett. **59,** 25 (1991).
15. J. E. Pedersen, V. G. Lyssenko, J. M. Hvam, P. H. Jepsen, S. R. Keiding, C. B. Sorensen, and P. E. Lindelof, Appl. Phys. Lett. **62,** 1265 (1993).